Journal of Physics: Conference Series

PAPER • OPEN ACCESS

Elaborated Modeling of Synchrotron Motion in Vlasov-Fokker-Planck Solvers

To cite this article: Patrik Schönfeldt *et al* 2018 *J. Phys.: Conf. Ser.* **1067** 062025

IOP Conf. Series: Journal of Physics: Conf. Series **1067** (2018) 062025 doi:10.1088/1742-6596/1067/6/062025

Elaborated Modeling of Synchrotron Motion in Vlasov-Fokker-Planck Solvers

Patrik Schönfeldt[1], Tobias Boltz[1], Akira Mochihashi[1], Johannes Leonard Steinmann[1] and Anke-Susanne Müller[1]

[1] Karlsruhe Institute of Technology , Karlsruhe, Germany

E-mail: patrik.schoenfeldt@kit.edu

Abstract. Solving the Vlasov-Fokker-Planck equation is a well-tested approach to simulate dynamics of electron bunches self-interacting with their own wake-field. Typical implementations model the dynamics of a charge density in a damped harmonic oscillator, with a small perturbation due to collective effects. This description imposes some limits to the applicability: Because after a certain simulation time coherent synchrotron motion will be damped down, effectively only the incoherent motion is described. Furthermore – even though computed – the tune spread is typically masked by the use of a charge density instead of individual particles. As a consequence, some effects are not reproduced. In this contribution, we present methods that allow to consider single-particle motion, coherent synchrotron oscillations, non-linearities of the accelerating voltage, higher orders of the momentum compaction factor, as well as modulations of the accelerating voltage. We also provide exemplary studies - based on the KIT storage ring KARA (KArlsruhe Research Accelerator) - to show the potentiality of the methods.

1. Introduction

When it comes to the simulation of beam dynamics in the longitudinal phase space of electron storage rings, the Vlasov-Fokker-Planck equation

$$\frac{\partial\psi}{\partial t}+\frac{\partial H}{\partial p}\frac{\partial\psi}{\partial q}-\frac{\partial H}{\partial q}\frac{\partial\psi}{\partial p}=\frac{2}{\tau_\mathrm{d}}\frac{\partial}{\partial p}\left(p\psi+\frac{\partial\psi}{\partial p}\right) \tag{1}$$

allows an elegant formulation of the self-interaction of the bunch with its own wakefield. It describes the evolution of the particle density $\psi(q,p)$, here using the generalized coordinates $q=z/\sigma_{z,0}$, and $p=(E-E_0)/\sigma_{\delta,0}$, and the Hamiltonian H. The quantities z, E, E_0, τ_d, $\sigma_{\delta,0}$, and $\sigma_{z,0}$ describe the longitudinal position, the energy, the reference particle's energy, the longitudinal damping time, the energy spread, and bunch length, respectively. The latter two exist in the equilibrium state at small bunch charges. The perturbation due to the collective effects is described as a perturbation to the Hamiltonian, which can be expressed in terms of an impedance $Z(\omega)$. To follow this approach, an ultra-relativistic ($\beta=1$, but $\gamma<\infty$) line charge is assumed.

In general, the evolution of the phase space can be expressed using a map

$$M:\psi(q,p,t)\rightarrow\psi(q,p,t+\Delta t). \tag{2}$$

IOP Conf. Series: Journal of Physics: Conf. Series **1067** (2018) 062025 doi:10.1088/1742-6596/1067/6/062025

Table 1. Physical parameters used for the simulations

Quantity	Symbol	Value	Unit
Accelerating Voltage	V_{RF}	799	kV
Beam energy	E_0	1.285	GeV
Energy spread	σ_E	6040	keV
Bending radius	R	5.559	m
Damping time	τ_{d}	10.4	ms
Harmonic number	h	184	
Revolution frequency	f_{rev}	2.716	MHz
Synchrotron frequency	$f_{\mathrm{s},0}$	8.27	kHz
Full beam pipe height	g	32	mm

For numerical stability, the map M can be split into a series of symplectic maps that are solutions to different parts of Eq. (1): A rotation (R) solves the unperturbed, conservative problem and the additional potential due to collective effects is modeled as an energy kick K. Damping and diffusion (RHS) are added in the spirit of a particular solution, and expressed by the non-symplectic map D. They are sequentially evaluated, so in total

$$M = D \circ K \circ R. \tag{3}$$

The application of the method for studying electron beam dynamics was first suggested by Warnock and Ellison [1] in 2000, and has since proven to show good convergence (e.g. [2, 3]). By splitting the rotation into an energy dependent drift followed by a location dependent RF kick [4]

$$R = R_{\mathrm{K}} \circ R_{\mathrm{D}}, \tag{4}$$

numerical stability can be further improved. An implementation of the features discussed in this paper can be found at [5], scripts to reproduce the results at [6]. The parameters used for the simulations are listed in Table 1. For the wake-field, we consider coherent synchrotron radiation shielded by parallel plates [7].

2. Passive particle tracking

As a charge density is considered, Vlasov-Fokker-Planck solvers do not need to reproduce the trajectories of individual particles. To still retrieve this information without the need to track a number of macro-particles that can represent the charge density with sufficient accuracy, we suggest passive particle tracking. Equation 2 can be expressed as [1]

$$\psi(r, t + \Delta t) \approx \psi(M(t|t + \Delta t)_{\psi(t)}(r), t), \tag{5}$$

where $M(t|t + \Delta t)_{\psi(t)}$ is a map that varies as ψ evolves in time. This notation mirrors the fact that it was evolved from

$$r' = M(t + \Delta t|t)(r), \tag{6}$$

which implies that a trajectory passing through r at time t passes through r' at time $t + \Delta t$. Calculating the maps based on the charge density provides good numerical stability, so we derive them using the charge density and afterwards express them in terms of the change of a particle's position and energy. To get a realistic picture, special care is needed for D: This map contains

IOP Conf. Series: Journal of Physics: Conf. Series **1067** (2018) 062025 doi:10.1088/1742-6596/1067/6/062025

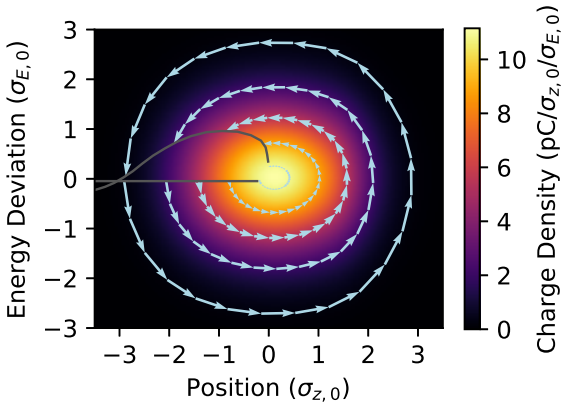

Figure 1. Example charge density of a bunch in the potential well distortion. Trajectories of five particles (light blue arrows) for a time corresponding to one unperturbed synchrotron period are displayed as an overlay. Also, there are two dark gray lines added that connect the positions at the first and the last time step, respectively. The dynamics have been calculated using the maps obtained based on the charge density, neglecting stochastic effects.

averaged quantum effects, which do not make sense on a single particle level. A first order probabilistic approach including both, damping and radiation excitation, is [8]

$$D : p(t + \Delta t) = p(t) \times \left(1 - \frac{2\Delta t}{\tau_\mathrm{d}}\right) + 2\sqrt{\frac{\Delta t}{\tau_\mathrm{d}}}\mathcal{N}\left(\sigma_p\right), \tag{7}$$

where $\mathcal{N}(\sigma)$ is a random number drawn from a zero-centered Gaussian distribution with the width σ. However, as the tracking is only performed for visualization purposes, it is also valid to think of an "average particle". An example using this flavour of the passive tracking method is shown in Fig. 1. It diplays the trajectories of five particles as an overlay to the charge density of an electron bunch in a distorted potential well. Using this method, tune spread and tune shift due to collective effects are clearly visible.

3. Dynamic accelerating voltage

Typically, the unperturbed LHS of Eq. (1) is evaluated to the first order, yielding a harmonic oscillator which is then modeled using the rotation map R. A time-dependent acceleration could in principle be modeled by adding a driving term to the RHS. We, instead, use the fact that we split R into two contributions [see Eq. (4)] parallel to the two dimensions that span the phase space. This way, only the RF kick map R_K has to be modified. For small variations, the phase modulation results in an additive term δ_+, the amplitude modulation in a multiplicative term $\delta_\times$ [9]. So the map can be expressed as

$$R_\mathrm{K} : p(q, t + \Delta t) = p(t) + \delta_+(t) + q \times \tan^{-1}(1/(\Delta t f_{\mathrm{s},0})) \times [1 + \delta_\times(t)], \tag{8}$$

with the synchrotron frequency $f_{\mathrm{s},0}$. For the unperturbed case ($\delta = 0$), the map is constant in t. So, the formulation is equivalent to a simple rotation for this unperturbed case.

As a first test, we consider Gaussian white noise to the RF phase. To do so, it has to be considered that the length of the time step Δt for the numerical solution of Eq. (1) can be arbitrarily chosen. So, the random distribution is sampled more often for small Δt. This can be compensated by introducing a correction factor [10] that scales the dynamics to be equal to

IOP Conf. Series: Journal of Physics: Conf. Series **1067** (2018) 062025 doi:10.1088/1742-6596/1067/6/062025

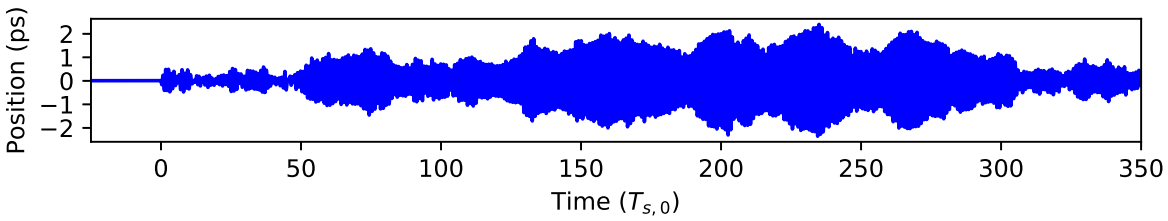

Figure 2. Evolution of the synchrotron oscillation amplitude over time. First, the simulated RF is stable. At $T = 0$, white Gaussian phase noise with $\sigma_q = 0.1° = 0.56\,\mathrm{ps}$ is turned on. The natural rms bunch length is $\sigma_{\mathrm{z},0} = 4.61\,\mathrm{ps}$.

the case where acceleration happens once per revolution period. In total

$$\delta_+ = \sqrt{\Delta t f_{\mathrm{rev}}} \times \mathcal{N}\left(\sigma_{\mathrm{q}}\right), \tag{9}$$

where σ_{q} is the RF phase spread σ_ϕ expressed in multiples of the natural bunch length. An example of simulation using $\sigma_\phi = 0.1°$ is displayed in Fig. 2. The RF phase noise drives a coherent synchrotron oscillation with stochastically varying amplitude. Its long-term mean amplitude is strongly dependent on the amplitude of the phase noise and can be calculated by [9]

$$\langle \phi^2 \rangle = \pi^2 f_{\mathrm{s},0}^2 \, \sigma_\phi^2 \, \tau_{\mathrm{d}} / f_{\mathrm{rev}}. \tag{10}$$

In a second step, we add RF amplitude noise with

$$\delta_\times = \sqrt{\Delta t f_{\mathrm{rev}}} \times \mathcal{N}\left(\sigma_{\mathrm{V}} / V_{\mathrm{RF}}\right), \tag{11}$$

where σ_{V} is the spread of the peak accelerating voltage. Bursting spectrograms of exemplary results are displayed in Fig. 3. In general, the simple model only considering the CSR impedance shielded by parallel plates reproduces the main features: There are strong frequency lines at $f \approx 30\,\mathrm{kHz}$ and its multiples as well as the occurrence of low frequency fluctuations at higher currents. The threshold currents, however, differ by $\approx 25\,\mu\mathrm{A}$. Introducing noise does not change this. Instead, it influences the background level in two ways: Without noise, the CSR ceases fluctuating below the threshold current. Considering noise removes this artifact. Furthermore, it actually lowers the noise floor between the two main frequency components. In the given example, this allows to see an additional structure at $f \approx 50\,\mathrm{kHz}$, which seems comparable to similar features in the measurement data. The simulated lines at the 2nd and 4th $f_{\mathrm{s},0}$ harmonic are due to asymmetries driven by the RF noise. In the projection to the profile, they appear with multiples $f_{\mathrm{s},0}$. The $f_{\mathrm{s},0}$ line in the measurement might be explained by the different transmission from the emitted light to the detector for different dispersive paths. In contrast, only emission is considered for the simulation. The difference in the instability threshold not being explained by noise suggests to take additional impedances into account.

In principle, Eq. (8) also holds for intentional RF modulations. However, they are typically driven with an amplitude [13–16] where the applicability of the linear approximation might be questioned. So, for these cases, the sinusoidal shape of the accelerating voltage should be considered. It can be expressed as

$$R_{\mathrm{K}} : p(t + \Delta t) = p(t) - f_{\mathrm{rev}} \Delta t \; e \; [V_{\mathrm{RF}} \sin(\omega_{\mathrm{V}} \; q(t) + q_0) + V_0] / \sigma_{\delta,0}, \tag{12}$$

where q_0 is the synchronous phase, ω_{V} is the RF frequency in units of q, and eV_0 is radiation loss of an electron per turn. When $(\omega_{\mathrm{V}} \; q(t) + q_0) \approx 0$, this formulation is equivalent to the linear approximation.

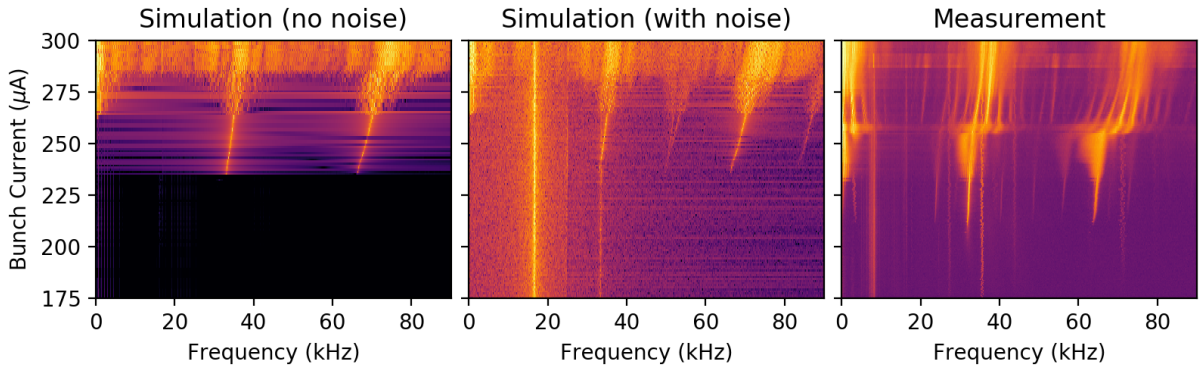

Figure 3. Spectrograms of emitted bursting coherent synchrotron radiation (see e.g. [11]). Left: Simulation data without RF noise. Center: Simulation considering RF phase noise with $\sigma_q = 0.01°$ and RF amplitude noise of $\sigma_V/V = 1\,\%$. Right: Measurement data obtained using a broad-band Schottky diode from ACST [12]. Both simulations reproduce the main frequency at $f \approx 30\,\mathrm{kHz}$ and its harmonics. The instability threshold is $211\,\mu\mathrm{A}$ for the measurement and $237\,\mu\mathrm{A}$ for both simulations. Adding noise improves the agreement between simulation and measurement in another aspect: The unphysical drop of the background at the lowest current disappears and the minimum intensity between the peak frequencies is lowered, where an additional structure becomes visible. (See text for interpretation of current-independent $f_{\mathrm{s},0}$ harmonics.)

4. Nonlinear momentum compaction

To complete the picture, we also include higher orders of the momentum compaction factor

$$\alpha_\mathrm{c} = \sum_{n=0}^{\infty} \alpha_n \left(\frac{E}{E_0}\right)^n = \frac{\Delta L/L_0}{\Delta E/E_0}, \tag{13}$$

where L_0 marks the length of the design orbit and ΔL the difference in orbit length due to an energy offset ΔE. This nonlinearity introduces a tune-spread that can e.g. Landau damp instabilities [2]. The modified drift map R_D now reads

$$R_\mathrm{D} : q(t + \Delta t) = q(t) + \eta_\mathrm{c}' \times p(t), \tag{14}$$

where $\eta_\mathrm{c}' = \alpha_\mathrm{c}' - 1/\gamma^2$ is the slip factor in the q, p coordinates. If $\alpha_n = 0\ \forall n > 0$, the map is identical to the one originally developed for the rotation.

5. Summary and outlook

We presented additions to Vlasov-Fokker-Planck solvers that allow to solve problems that were previously not addressed by this simulation method. As a premiere example, we considered RF noise. In the simulation of bursting CSR, the addition allows to see frequency components that where not reproduced before. Systematic studies modeling intentional RF phase modulation and using nonlinear momentum compaction are planned and first tests already show promising results.

6. Acknowledgments

Funded by the German Federal Ministry of Education and Research (Grant No. 05K16VKA) and Initiative and Networking Fund of the Helmholtz Association (contract number: VH-NG-320). T. Boltz, P. Schönfeldt and J. L. Steinmann want to acknowledge the support by the Helmholtz International Research School for Teratronics (HIRST).

References

[1] Warnock R L and Ellison J A 2000 A general method for propagation of the phase space distribution, with application to the sawtooth instability Tech. Rep. SLAC-PUB-8404 SLAC

[2] Bane K L F, Cai Y and Stupakov G 2010 *Phys. Rev. ST Accel. Beams* **13**(10) 104402

[3] Roussel E, Evain C, Szwaj C and Bielawski S 2014 *Phys. Rev. ST Accel. Beams* **17**(1) 010701 URL `https://link.aps.org/doi/10.1103/PhysRevSTAB.17.010701`

[4] Schönfeldt P, Brosi M, Schwarz M, Steinmann J L and Müller A S 2017 *Phys. Rev. Accel. Beams* **20**(3) 030704 URL `link.aps.org/doi/10.1103/PhysRevAccelBeams.20.030704`

[5] Schönfeldt P, Blaicher M, Boltz T and Schreiber P 2018 Inovesa source code URL `https://github.com/Inovesa/Inovesa`

[6] Schönfeldt P and Brosi M 2018 Inovesa examples URL `https://github.com/Inovesa/examples`

[7] Murphy J, Krinsky S and Gluckstern R 1997 *Particle Accelerators* **57** 9–64 URL `http://cds.cern.ch/record/1120287/files/p9.pdf`

[8] Bane K L F and Oide K 1993 Simulations of the longitudinal instability in the slc damping rings *Proceedings of International Conference on Particle Accelerators* vol 5 pp 3339–3341

[9] Ormond K W and Rogers J T 1997 Synchrotron oscillation driven by rf phase noise *Proceedings of the 1997 Particle Accelerator Conference (Cat. No.97CH36167)* vol 2 pp 1822–1824 vol.2

[10] Schestag J 2018 *Study of Noise in the Simulation of Collective Effects of Releativistic Electron Bunches* Bachelor's thesis Karlsruhe Institute of Technology

[11] Brosi M, Steinmann J L, Blomley E, Bründermann E, Caselle M, Hiller N, Kehrer B, Nasse M J, Rota L, Schedler M, Schönfeldt P, Schuh M, Schwarz M, Weber M and Müller A S 2016 *Phys. Rev. Accel. Beams* **19**(11) 110701 URL `link.aps.org/doi/10.1103/PhysRevAccelBeams.19.110701`

[12] ACST GmbH 2017 Quasi-optical detectors URL `http://www.acst.de/`

[13] Huang H, Ball M, Brabson B, Budnick J, Caussyn D D, Chao A W, Collins J, Derenchuk V, Dutt S, East G, Ellison M, Friesel D, Hamilton B, Jones W P, Lee S Y, Li D, Minty M G, Nagaitsev S, Ng K Y, Pei X, Riabko A, Sloan T, Syphers M, Teng L, Wang Y, Yan Y T and Zhang P L 1993 *Phys. Rev. E* **48**(6) 4678–4688 URL `https://link.aps.org/doi/10.1103/PhysRevE.48.4678`

[14] Orsini F and Mosnier A 2000 *Phys. Rev. E* **61**(4) 4431–4440 URL `https://link.aps.org/doi/10.1103/PhysRevE.61.4431`

[15] Abreu N P, Farias R H A and Tavares P F 2006 *Phys. Rev. ST Accel. Beams* **9**(12) 124401 URL `https://link.aps.org/doi/10.1103/PhysRevSTAB.9.124401`

[16] Jebramcik M *et al.* 2016 Coherent Harmonic Generation in the Presence of Synchronized RF Phase Modulation at DELTA *Proc. of International Particle Accelerator Conference (IPAC'16), Busan, Korea, May 8-13, 2016* (*International Particle Accelerator Conference* no 7) (Geneva, Switzerland: JACoW) pp 2847–2850 ISBN 978-3-95450-147-2 URL `http://jacow.org/ipac2016/papers/wepow013.pdf`